

FATIGUE CRACK GROWTH IN MODE II OF ADHESIVELY JOINED COMPOSITES

Anders Biel¹ and Helmuth Toftegaard²

¹Section of Composites and Materials Mechanics, Department of Wind Energy, Technical University of Denmark, 399, DK-4000 Roskilde, Denmark

Email: abie@dtu.dk, Web Page: <http://www.dtu.dk>

²Section of Composites and Materials Mechanics, Department of Wind Energy, Technical University of Denmark, P.O. Box 49, Frederiksborgvej 399, DK-4000 Roskilde, Denmark

Email: heto@dtu.dk, Web Page: <http://www.dtu.dk>

Keywords: fatigue, fracture, adhesive, experiment, shear

Abstract

The structure of a wind turbine is exposed to a complex multi-axial cyclic loading. The blades are commonly manufactured of adhesively joined composites. Adhesive joints are usually strongest if loaded in shear and accordingly fatigue properties in shear are important.

In the current paper, experiments are performed to derive material data for a crack propagation in shear i.e. in mode II. The shear loading of the crack is achieved by use of *double cantilever beam* specimens loaded with *uneven bending moments*. The experiments are performed under a constant cyclic displacement. An initial mode I loading is used to make the crack start in the adhesive. The crack length is measured using a load synchronized camera.

Due to the shear loading the crack deviates from the adhesive layer into the laminate. A stable crack propagation is detected in the laminate. No influence have been detected due to an increasing crack length. It is also observed that the crack is trapped in the laminate; if the loading is changed to mode I the crack continues to propagate in the laminate.

1. Introduction

The desired lifetime for wind turbines is 20 years or about $5 \cdot 10^8$ load cycles. This desired fatigue limit is far beyond common lifetime predictions and the loading conditions are complex. The rotor blades of a modern wind turbine are manufactured of adhesively joined composites. In comparison with other joining methods like screws or rivets, adhesive joints are preferably since they distribute the load over a larger area. However, to obtain improved performance the mechanical properties of the adhesive joint have to be adapted for the current situation. To this date, design tools for adhesive joints still need to be developed.

The loading on an adhesive joint can be divided into two parts, normal stress, σ , and shear stress, τ , see Fig 1. The corresponding displacements are δ_n and δ_s . Adhesive joints are usually strongest if loaded in shear, cf. e.g. [1, 2]. Three different types of failures are associated with adhesive joints, viz. *cohesive failure* (fracture in the adhesive), *adhesive failure* (fracture between adhesive and substrate) and *failure in the substrate*. The kind of failure is dependent on material properties and loading conditions, and combinations of different failure types are common.

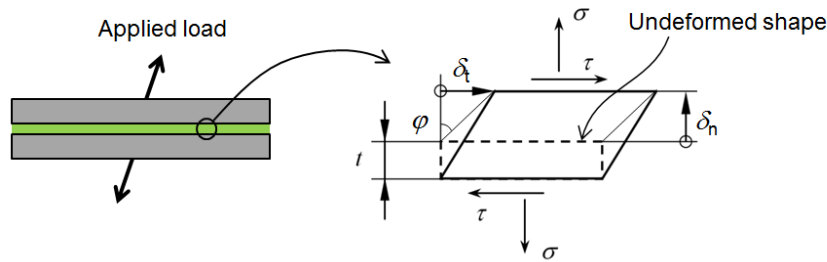


Figure 1. Loading of an adhesive layer.

A recent study shows that the joint at the *trailing edge* (TE) is one of the most critical positions in a rotor blade; see Fig 2a [3]. The inner part of the joint is more severely loaded than the outer part. A fatigue crack can be expected to start in this position and propagate along the edge, see Fig 2b.

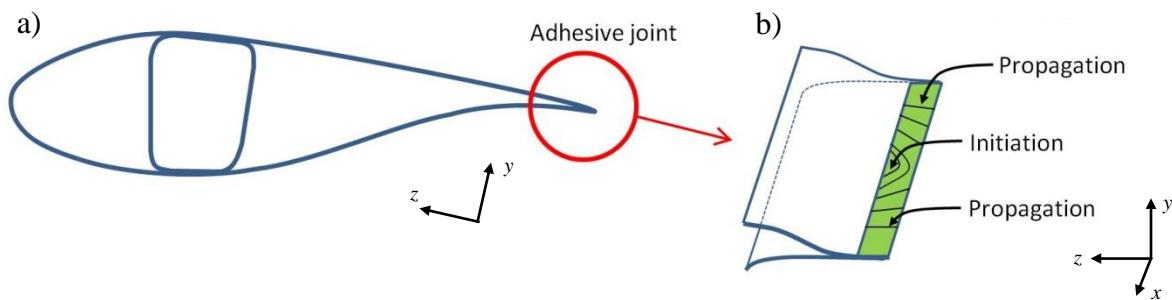


Figure 2. a) Schematic cross-section and b) crack initiation and propagation at the trailing edge.

Figure 3 shows the TE from a blade (SSP 34 m) which has failed due to one single overload. Several slanted cracks are visible. The slanted cracks in the 45° direction indicate the presence of a shear load, cf. e.g. [4]. The final failure is close to the interface, however, a mixture of cohesive failure, adhesive failure and failure in the substrate (composite) are observed. In this paper, experiments are performed in order to determine shear fatigue properties of adhesively joined composites.

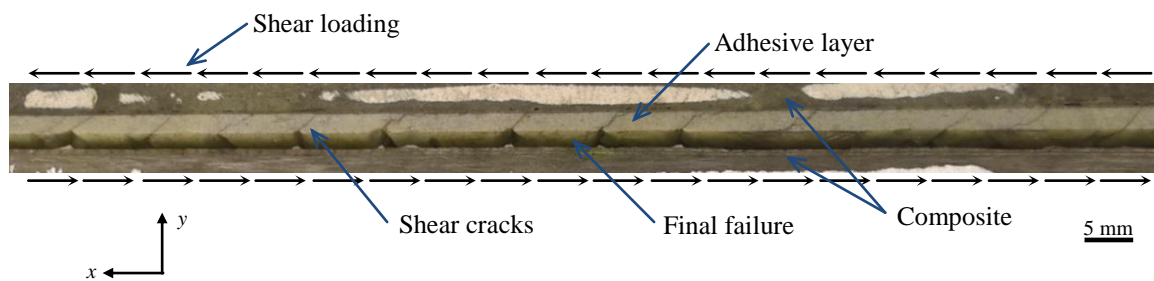


Figure 3. Shear cracks and failure observed in a 34 m SSP-blade.

2. Method

In this study, we utilize the *double cantilever beam* specimen (DCB) and methods based on the *J*-integral approach [5]. The general geometry and the loading are shown in Fig. 4.

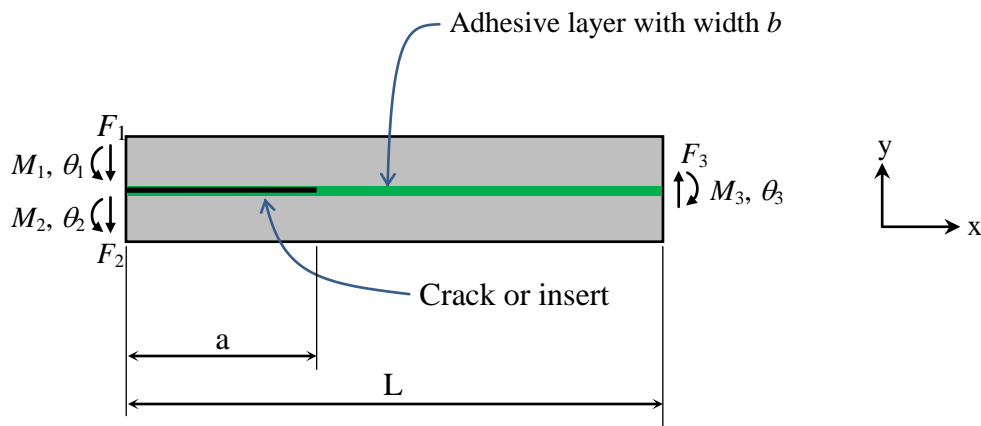


Figure 4. Loading for a DCB-specimen.

The DCB-specimen can be loaded with forces [6, 7] or with moments [8, 9]. It is possible to superimpose the two cases. A summary of present methods to calculate the energy release rate is given in [10]. During fracture propagation, the energy release rate equals the fracture energy. Two common ways to achieve pure shear exists, viz. by *three point bending* specimen or by *four point bending* specimen. The three point bending specimen for fracture is usually named *end notched flexure* specimen (ENF). Pure shear is achieved if the specimen is loaded by, $F_1 = F_2 = F_3/2$, $M_3 = F_3L$ and $M_1 = M_2 = 0$. The four point bending specimen is a special case of the *double cantilever beam with uneven bending moments* (DCB-UBM). Pure shear is achieved if the specimen is loaded by, $F_1 = F_2 = F_3 = 0$ and $M_1 = M_2 = M_3/2$. The latter method is used in this study. It is used in several previous studies, cf. e.g. [11]. The method has also been used for fatigue of laminates, see [12].

3. Specimens and experiments

The DCB-specimens are manufactured from GRFP-plates with a thickness of $h = 8$ mm. The plates are joined by a $t = 3$ mm thick adhesive. After curing, the plates are cut to desired geometry; $b = 30$ mm, $a = 70$ mm and $L = 0.5$ m, see Fig. 5. An insert foil is used to create a start for the crack propagation. Taps are attached to the specimen for an easy introduction of the loads.

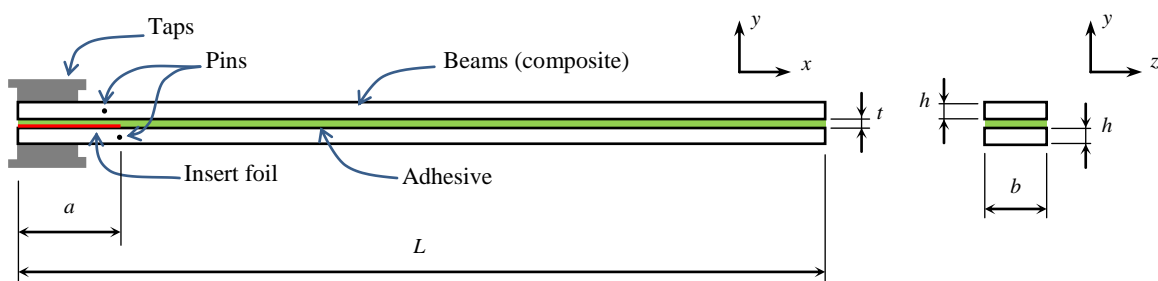


Figure 5. Geometry of the used DCB-specimen.

A specially designed servo hydraulic test frame is used to apply the fatigue load by pure bending moments. The load is applied to the specimen by wires and lever arms, see sketch in Fig. 6a. The equipment has been used in earlier studies, see e.g. [12]. In this study, the equipment is complemented with a load synchronized camera which is used to measure the crack growth. The camera takes pictures at predefined load cycles. The surface of the specimen is painted white in order to increase the visibility of the cracks. A special light source is used in order to have a uniform illumination.

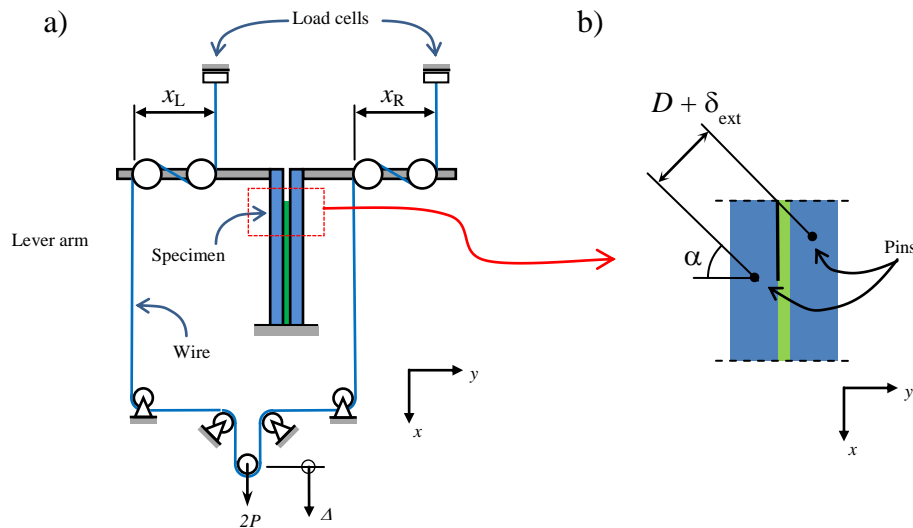


Figure 6. a) Sketch of the experimental setup and b) measurement of the displacement.

The load is controlled by an extensometer, which is attached to two pins, see Fig 6b. The pins are oriented at a distance $D = 15$ mm at an angle of $\alpha = 45^\circ$. The slanted orientation is done in order to increase the sensitivity to the shear deformation. The applied moments are $M_1 = PX_R$ and $M_2 = PX_L$, where P is the force in the wire. Two load cells are used to measure the force in the wire, see Fig 6a. A mean value of these is used in the evaluation. A sharp crack tip is achieved by an initial loading in mode I.

During the experiments the amplitude of the extensometer opening is kept at a constant level, $\Delta\delta_{ext} = \delta_{max} - 0.2\delta_{max}$, see Fig 7a. The lower value, $0.2\delta_{max}$, is needed in order to avoid zero forces in the wire. The relation between the applied energy release rate i.e. the moment and the deformation at the extensometer, δ_{ext} , is evaluated during a preload. The initial load level, δ_{max} is adjusted to give a load level, ΔJ , below the load, ΔJ_{max} , which gives failure for quasi static experiments of the laminate.

Crack growth will give a decreased loading (moment), see Fig. 7b. The decreased load will give a decrease in the crack growth rate and accordingly one single experiment will cover a large span of grow rates. When a threshold level is reached and no further crack growth is detected, it is possible to restart the experiment by using new settings for the extensometer opening i.e. one specimen can be used for several experiments.

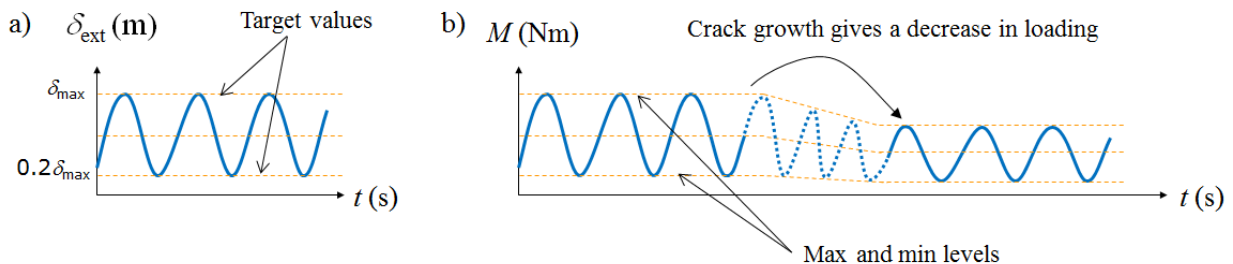


Figure 7. a) Applied displacement and b) decrease in applied load due to increased crack length.

The experiments are performed with almost pure mode II loading. However, a small amount of mode I loading is also applied in order to avoid friction between the crack surfaces. Two things have an influence on the mode mix; (1) different lengths of the lever arms ($X_L = 108$ mm, $X_R = 105$ mm) and (2) a slightly unsymmetrical specimen due to the position of the crack.

3. Results and conclusions

Four experiments are performed and evaluated. The cyclic loading is applied with a frequency of 1 Hz. The maximum number of cycles used in the experiments is $1 \cdot 10^6$ cycles. For all experiments the fatigue crack is propagating in the laminate close to the adhesive layer. Figure 8 shows the growth rate vs. the load. The growth rate da/dN decreases with a decreasing load; at 60% of ΔJ_{\max} the growth rate is about $1 \cdot 10^{-2}$ mm/cycle and at 15% of ΔJ_{\max} the growth rate is about $1 \cdot 10^{-5}$ mm/cycle. No clear lower threshold level has been found. The measurement at low loads are more uncertain. The crack opens less which makes it harder to measure the correct crack length.

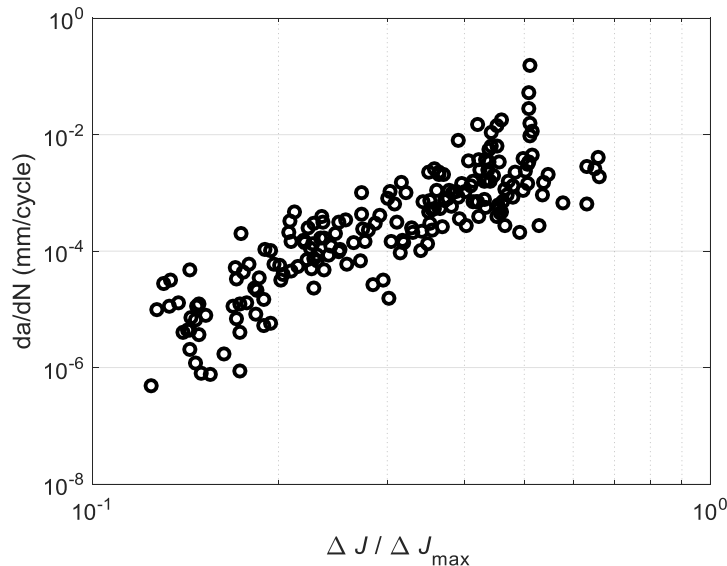


Figure 8. Fatigue crack propagation in mode II.

Figure 9 shows the one of the images used to measure the crack length. The experiments have different crack lengths; no influence of crack length is observed. The first part of the crack, is created by an initial loading in mode I. During this part the crack propagates in the adhesive. When the loading is changed to mode II (shear) the crack directly deviates in to the laminate. The crack follows one layer in the laminate close to adhesive layer. For one experiment, the fatigue loading was changed from mode II to mode I. Although the changed loading the fatigue crack continue to propagate in the laminate. Thus, the fatigue properties of the joint is dependent on the loading history.

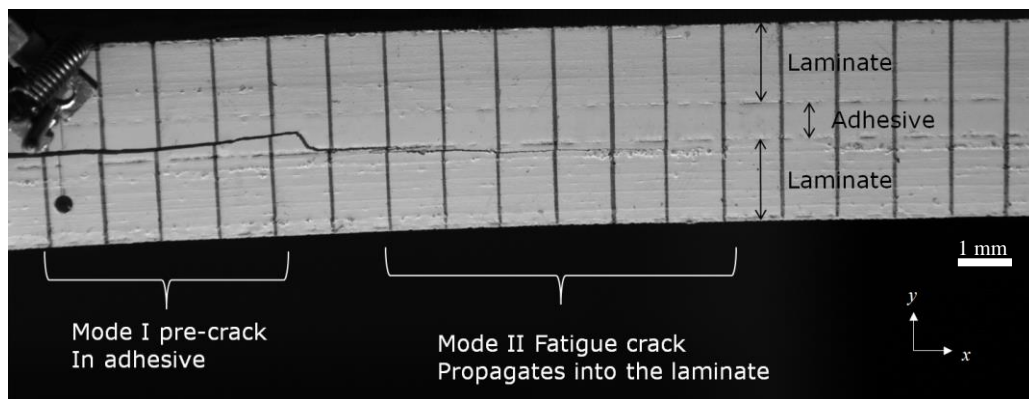


Figure 9. Image of crack propagation in the specimen.

References

- [1] A.J. Kinloch. *Adhesion and adhesives: Science and technology*. Chapman and Hall, 1987.
- [2] U. Stigh, A. Biel and T. Walander. Shear strength of adhesive layers - Models and experiments. *Engineering Fracture Mechanics*, 129:67-76, 2014.
- [3] P.U. Haselbach, M.A. Eder and F. Belloni. A comprehensive investigation of trailing edge damage in a wind turbine rotor blade. *Wind Energy* 2016.
- [4] H. Chai. Shear fracture. *International Journal of Fracture*, 37:137-159, 1988.
- [5] J.R. Rice. A Path Independent Integral and the Approximate Analysis of Strain Concentration by Notches and Cracks. *Journal of Applied Mechanics Transactions of the Asme*, 35:379-386, 1968.
- [6] A.J. Paris and P.C. Paris. Instantaneous evaluation of J and C*. *International Journal of Fracture*, 38:R19-21, 1988.
- [7] T. Andersson and U. Stigh. The stress-elongation relation for an adhesive layer loaded in peel using equilibrium of energetic forces. *International Journal of Solids and Structures*, 41:413-434, 2004.
- [8] Z. Suo, G. Bao and B. Fan. Delamination R-curve phenomena due to damage. *Journal of the Mechanics and Physics of Solids*, 40:1-16, 1992.
- [9] B.F. Sørensen. Cohesive law and notch sensitivity of adhesive joints. *Acta Metallurgica Materialia*, 50:1053-1061, 2002
- [10] U. Stigh, K.S. Alfredsson, T. Andersson, A. Biel, T. Carlberger and K. Salomonsson. Some aspects of cohesive models and modelling with special application to strength of adhesive layers. *International Journal of Fracture*, 165:149-162, 2010.
- [11] B.F. Sørensen, K. Jørgensen, T.K. Jacobsen and R.C. Østergaard. DCB-specimen loaded with uneven bending moments. *International Journal of Fracture*, 141:163-176, 2006.
- [12] J.W. Holmes, L. Liu, B.F. Sørensen and S. Wahlgren. Experimental approach for mixed-mode fatigue delamination crack growth with large-scale bridging in polymer composites. *Journal of Composite Materials*, 48:3111-3128, 2014.